Performance evaluation of nonchemically amplified negative tone photoresists for e-beam and EUV lithography

Vikram Singh
Vardhineedi Sri Venkata Satyanarayana
Nikola Batina
Israel Morales Reyes
Satinder K. Sharma
Felipe Kessler
Francine R. Scheffer
Daniel E. Weibel
Subrata Ghosh
Kenneth E. Gonsalves

SPIE.

Performance evaluation of nonchemically amplified negative tone photoresists for e-beam and EUV lithography

Vikram Singh,[a] Vardhineedi Sri Venkata Satyanarayana,[b] Nikola Batina,[c] Israel Morales Reyes,[c] Satinder K. Sharma,[a] Felipe Kessler,[d] Francine R. Scheffer,[d] Daniel E. Weibel,[d] Subrata Ghosh,[b,*] and Kenneth E. Gonsalves[b,*]

[a]Indian Institute of Technology Mandi, School of Computing and Electrical Engineering, Mandi, Himachal Pradesh 175001, India
[b]Indian Institute of Technology Mandi, School of Basic Sciences, Mandi, Himachal Pradesh 175001, India
[c]Depto. de Química, Lab. de Nanotecnología e Ingeniería Molecular, CBI, UAM-I, Mexico D.F., Mexico
[d]Universidade Federal do Rio Grande do Sul, UFRGS, Instituto de Química, Avenida Bento Gonçalves 9500, P.O. Box 15003, 91501-970 Porto Alegre, RS, Brazil

Abstract. Although extreme ultraviolet (EUV) lithography is being considered as one of the most promising next-generation lithography techniques for patterning sub-20 nm features, the development of suitable EUV resists remains one of the main challenges confronting the semiconductor industry. The goal is to achieve sub-20 nm line patterns having low line edge roughness (LER) of <1.8 nm and a sensitivity of 5 to 20 mJ/cm^2. The present work demonstrates the lithographic performance of two nonchemically amplified (n-CARs) negative photoresists, MAPDST homopolymer and MAPDST-MMA copolymer, prepared from suitable monomers containing the radiation sensitive sulfonium functionality. Investigations into the effect of several process parameters are reported. These include spinning conditions to obtain film thicknesses <50 nm, baking regimes, exposure conditions, and the resulting surface topographies. The effect of these protocols on sensitivity, contrast, and resolution has been assessed for the optimization of 20 nm features and the corresponding LER/line width roughness. These n-CARs have also been found to possess high etch resistance. The etch durability of MAPDST homopolymer and MAPDST-MMA copolymer (under SF$_6$ plasma chemistry) with respect to the silicon substrate are 7.2 : 1 and 8.3 : 1, respectively. This methodical investigation will provide guidance in designing new resist materials with improved efficiency for EUVL through polymer microstructure engineering. © 2014 Society of Photo-Optical Instrumentation Engineers (SPIE) [DOI: 10.1117/1.JMM.13.4.043002]

Keywords: nonchemically amplified resist; postexposure bake; postapply bake; e-beam lithography; extreme ultraviolet lithography; surface roughness; contrast; sensitivity; etch resistance.

Paper 14069P received May 6, 2014; revised manuscript received Aug. 27, 2014; accepted for publication Sep. 4, 2014; published online Oct. 16, 2014.

1 Introduction

Extreme ultraviolet lithography (EUVL) using a 13.5-nm wavelength is considered to be one of the most promising candidates for next-generation lithography (NGL) technology.[1] One of the key challenges in EUVL is simultaneously meeting resist performance targets like sensitivity, resolution, etch resistance, and line edge roughness (LER).[2] It is known that chemically amplified resists (CARs) limit the ultimate minimum half-pitch (hp) resolution, especially for features at 20 nm and below due to their postexposure instability and acid diffusion problem.[3–6] In addition to these effects, LER or line width roughness (LWR) and critical dimension (CD) play a significant role in sub-20 nm technology and beyond which are not met by CARs, specifically with regard to the ITRS-2013 guidelines.[2,7–10] Although CARs have successfully been used for patterning down to 15 nm hp, their sensitivity (30 mJ/cm^2) still remains an issue.[10] It is known that for CARs, a decrease in hp for sub-20 nm technology leads to pattern collapse and, therefore, limits the resolution and LER. For these reasons, the above-stated requirements must be effectively controlled. Thus, an additional constraint has been superimposed on chemically amplified resists. Due to these shortcomings, recent attention has focused on the development of nonchemically amplified resists (n-CARs) with improved lithography performance capable of patterning both isolated and dense lines patterns to facilitate the high throughput production of equally isolated (IC logic gates) and dense (DRAM, FRAM memory) areas of devices for future successful implementation of NGL technology nodes.[11]

Herein, we investigated the novel n-CARs negative tone resists based on the copolymer poly(4-(methacryloyloxy) phenyldimethylsulfoniumtriflate-co-methylmethacrylate) [poly(MAPDST-co-MMA)], as well as the poly(4-(methacryloyloxy)phenyldimethylsulfoniumtriflate (MAPDST-homopolymer) that are prepared from monomers containing sulfonium groups. These polymeric resists are directly sensitive to radiation and function without utilizing the concept of chemical amplification. Novel n-CARs and process optimization, such as film thickness, spinning speed, effect of the prebake and postbake temperatures, etch resistance, electron beam lithography (EBL) exposure dose, surface topography, and morphology are reported here. The EUV performance and photodynamic studies of such nonchemically amplified (n-CAR) negative tone photoresists are reported, including

---

*Address all correspondence to: Subrata Ghosh, E-mail: subrata@iitmandi.ac.in; Kenneth E. Gonsalves, E-mail: kenneth@iitmandi.ac.in

the ultimate resolution, sensitivity, and low LER/LWR using the Microfield Exposure Tool (MET) at Berkeley. These results are aimed at providing a clear understanding of how the lithographic imaging process impacts the n-CA resist concept.

2 Materials and Methods

2.1 Materials

The monomer 4-(methacryloyloxy)phenyl)dimethylsulfonium triflate (MAPDST) was synthesized following the literature procedure.[12–16] The resist, poly(MAPDST-co-MMA), was synthesized using azobisisobutyronitrile (AIBN) initiated free radical cross-polymerization between MAPDST and MMA (1:1 molar feed ratio) at 60°C under a dry nitrogen atmosphere for two days. The molecular weight (M_w) of this copolymer was calculated to be 17.7×10^3 by gel permeation chromatography (GPC). The composition determined by ^{1}H NMR corresponds to $(MAPDST)_{75}(MMA)_{25}$. Similarly, an MAPDST homopolymer was synthesized by reacting monomer MAPDST and using AIBN as an initiator of 1 wt% relative to the monomer in acetonitrile at 60°C underneath a dry nitrogen atmosphere for two days. The molecular weights of this homopolymer ($M_w = 20.7 \times 10^3$) and copolymer ($M_w = 17,000$) were determined using GPC analysis. Chemical structures of these polymers are shown in Figs. 1(a) and 1(b). Both the resist materials were obtained as white powders. The synthesized resist materials were characterized using Fourier transform infrared spectroscopy, ^{1}H NMR, and differential scanning calorimetry and thermal gravimetric analysis.[17]

2.2 Thin Film Preparation for EBL Evaluation

The resist solution of the synthesized MAPDST homopolymer and poly(MAPDST-co-MMA) copolymer were prepared in methanol at 3% by weight of polymer and filtered through a 0.2-μm Teflon filter to remove particles. For e-beam evaluation, the thin films of the MAPDST homopolymer and poly(MAPDST-co-MMA) copolymer negative photoresist solutions were spin-coated directly on Radio Corporation of America cleaned bared Si wafers to ~30 to 60 nm thickness and then baked on a hot plate to remove any excess solvent. Exposures were carried out by using a Raith GmbH (Dortmund, Germany), 150-Two model machine (e-beam) at the exposure energy of 20 KeV by covering a broad range of doses. The exposed samples were

developed in optimized aqueous solutions of tetramethyl ammonium hydroxide (TMAH) (0.003 N) in de-ionized (DI) water maintained at a pH ~12 at room temperature, rinsed in de-ionized water, and blow dried with pure nitrogen gas. These polymers were also evaluated by EUV exposure at the SEMATECH-Berkeley MET lab.[18] The CD, LER, and LWR were calculated using SuMMIT® software.

Films were characterized by means of atomic force microscope (AFM) imaging using AFM (Multimode Nanoscope IV, Digital Instruments, Santa Barbara, California). Images were taken by a very slow scan rate of only 0.5 Hz in the tapping mode to avoid possible damaging of the patterns. In order to achieve a necessary nanoscale resolution, we used two types of AFM tips: the high aspect ratio tips with a 2-μm spike mounted at the end of the cantilever and DP15/HiRes-C/AIBS, with a tip apex of only 1 nm (MikroMasch, NanoAndMore, Soquel, California).

2.3 Thin Film Preparations for EUV Evaluation

For EUV evaluation, the MAPDST homopolymer and poly (MAPDST-co-MMA) copolymer negative tone resist solutions were prepared in methanol and filtered with a 0.2-micron Teflon filter then spin-coated onto an hexamethyldisilazane (HMDS) treated 200-mm silicon wafer for ~40-nm thin films. The thin films of the MAPDST homopolymer and poly(MAPDST-co-MMA) copolymer were prebaked at 100°C for 90 s and 90°C for 90 s, respectively. The respective center doses, as determined from initial test wafer exposures, were assessed to be ~90 mJ/cm^2 for the homopolymer and 30 mJ/cm^2 for the copolymer. It should be pointed out that the actual center dose value for the MAPDST homopolymer is not certain at this time. It is highly dependent on developer conditions, and more test runs are required for EUV optimizations. Based on these center doses, the resulting photoresist layers were flood exposed with the respective dose array using mask IMO228775 with a field of R_4C_3 at the SEMATECH Berkeley MET. The sample was postexposed baked at 115°C for 90 s and developed in optimized aqueous solutions of TMAH (0.003 N) in DI water to obtain high-resolution line patterns.

2.4 Photodynamic Studies

EUV photodynamic studies were carried out at the Brazilian Synchrotron Light Source (LNLS) Campinas. In these experiments, the planar grating monochromator (PGM) beam line for EUV, VUV, and soft x-ray spectroscopy (100 to 1500 eV), which gives a spectral resolution (E/ΔE) = 25,000, was used as the monochromatic photon source. The experimental setup includes a computer-controlled XYZ sample manipulator housed in an ultrahigh vacuum (UHV) chamber ($P{\sim}1 \times 10^{-9}$ mbar). The Si wafers were directly attached to the sample holder by using conducting double-sided tape and the synchrotron radiation (SR) beam was slightly defocused. No sample charging was observed throughout the experiments. Samples outside the UHV chamber were always manipulated in an inert atmosphere and ultraviolet light exposition was avoided. Resist films were characterized by x-ray photoelectron spectroscopy (XPS) using a high-performance hemispheric SPECSLAB II (Phoibos-Hs 3500 150 analyzer, SPECS, Berlin, Germany) energy analyzer. Additionally, a quadruple mass spectrometer (QMS, Pfeiffer compact mass spectrometer,
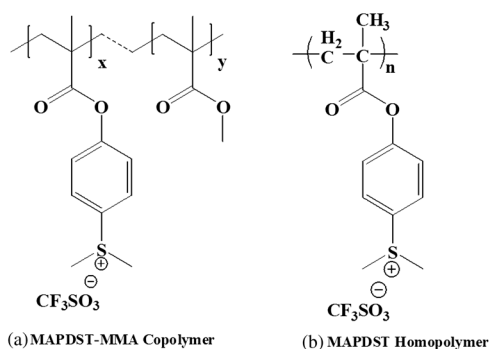

(a) **MAPDST-MMA Copolymer**   (b) **MAPDST Homopolymer**

Fig. 1 Chemical structures of (a) MAPDST-MMA copolymer ($x = 75\%$, $y = 25\%$) and (b) MAPDST homopolymer.

open ion source, 1–200 amu, Berlin, Germany) was integrated into the vacuum chamber. Additionally, a quadruple mass spectrometer (QMS) was integrated into the vacuum chamber in order to examine the volatile defragmentation products ablated from the irradiated polymer surface by an *in situ* gas analysis. When SR was used to irradiate the films (1 and 5 min), a specific energy was selected (103.5 eV) that corresponds to the maximum intensity of the ondolatory radiation at the PGM beam line. After irradiation, pure oxygen at atmospheric pressure was introduced into the UHV chamber for 30 min to neutralize the remaining radicals on the film surface. Please note that the above exposure energy was maintained to be as close as possible to that of the BMET tool.

2.5 Film Preparation for EUV Photodynamic Study

Samples were prepared by spin coating inside a glove box containing dry nitrogen gas (purity grade: 5.0) and under red light illumination. One of two drops of the resist solution was set on cleaned silicon wafers (0.5×1 cm).

3 Results and Discussions

3.1 E-Beam Evaluation and Postbake Condition

Upon irradiation of polymeric film using a Raith 150 e-beam lithography system at an energy of 20 KeV, a polarity difference in exposed and unexposed areas was observed. The unexposed MAPDST homopolymer was polar due to its ionic character and, therefore, was soluble in polar solvents, such as water. Unexposed regions of the MAPDST homopolymer negative tone resist film readily dissolved in an aqueous TMAH developer (0.003 N, pH 11.5), while the exposed patterns were maintained after dipping the exposed resist film in developer. These are characteristics of a nonchemically amplified negative polymeric resist. The MAPDST homopolymer exhibited 20-nm patterns (20KX magnification) at doses 20, 25, and 40 μC/cm^2 at various postbake conditions. These are as given in Fig. 2.

The postbake temperature was found to be very crucial for obtaining clear line patterns (the reason for the improved imaging results while using a postexposure bake has been discussed in Sec. 3.4). An attempt to develop 20-nm line patterns using a relatively low postbake temperature
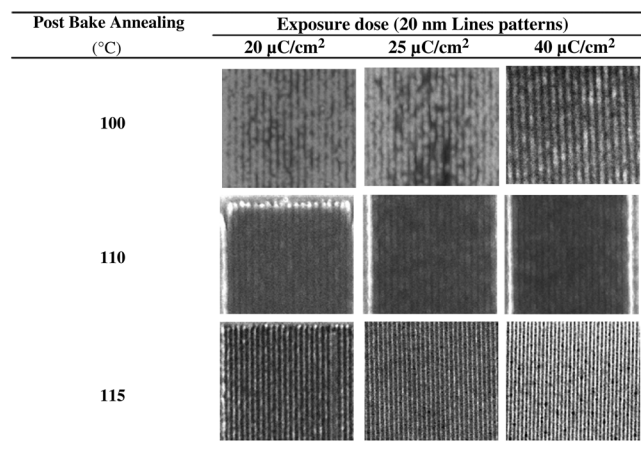

Post Bake Annealing	Exposure dose (20 nm Lines patterns)		
(°C)	20 μC/cm^2	25 μC/cm^2	40 μC/cm^2
100			
110			
115			

Fig. 2 E-beam lithography results, 20-nm features, for nonchemically amplified negative resist (MAPDST homopolymer) under different postbake conditions.

(100°C/90 s) failed completely when the films were exposed at lower doses (20 to 25 μC/cm^2). Some line patterns were observed at this postbake temperature only when the films were exposed at a higher dose (40 μC/cm^2) (Fig. 2). A slight increase in postbake temperature improved the patterning process and resulted in 20 nm features (Fig. 2). Finally, after an extensive investigation and gradual optimization of the postbake effect on the exposed resists, a protocol was developed for high-quality 20-nm line patterns of MAPDST homopolymer at 115°C/90 s. A similar protocol with a postbake condition of 100°C/90 s was adapted for the copolymer resist to obtain an improved pattern fidelity.

3.2 Contrast Analysis

The contrast curve of MAPDST homopolymer resist films was determined after the exposure of e-beam on a Raith 150 system at 20 KeV for varying doses ranging from 1 to 70 μC/cm^2 for 20×100 μm pads. After exposure, the resist was developed at various developing times (25, 21, and 17 s) by dipping the exposed films in optimized aqueous solutions of TMAH (0.003 N) in DI-water with a pH ~11.5 to 12, as shown in Fig. 3. The thickness of the developed patterns was measured on a Stylus profilometer. After developing for 17 s, a high contrast of $\gamma = 3.6$ with a sensitivity 5.25 μC/cm^2 was obtained. It is clearly shown in Fig. 3 that the contrast of the MAPDST homopolymer is highly dependent on the developing conditions.

High contrast (γ)/sensitivity (μC/cm^2) $-1.8/2.06$ for the MAPDST-MMA copolymer resist was also obtained as shown in Fig. 4. These are highly improved when compared with the e-beam dose values reported in the literature for other nCARs, such as AR-N7500,[17,19] maN2400,[17,20] HSQ,[21] and Fullerol.[22]

3.3 Surface Roughness of Developed Film

The surface roughness of the MAPDST homopolymer after e-beam exposure with various doses and using a 0.003 N TMAH base developing condition as stated above is shown in Fig. 5. The RMS values (AFM analysis) of the MAPDST homopolymer surface vary with the e-beam lithography exposure dose. It is clearly shown in Fig. 5 that roughness remains constant above 25 μC/cm^2. However, below this critical dose, roughness increases rapidly. Similarly, the critical dose for MAPDST-MMA copolymer was found to be 20 μC/cm^2. It appears that the optimum dose window is 20 to 60 μC/cm^2.

3.4 High-Resolution Patterning Using EUV Lithography

The EUV exposure results of the nonchemically amplified MAPDST homopolymer and MAPDST-MMA copolymer resists at the SEMATECH-Berkeley MET lab[18] are shown in Fig. 6. High-resolution lines patterns with high-quality scanning electron microscope images (at 120 K magnification) were obtained for both n-CAR materials having a low LER. The 20-nm lines with a 20 nm CD/40 nm pitch line space pattern of both the resist polymers are very clear and sharp at the edges.

The low LER was unambiguously confirmed by higher magnification (120 K magnification) field emission scanning electron microscopy images of the MAPDST homopolymer
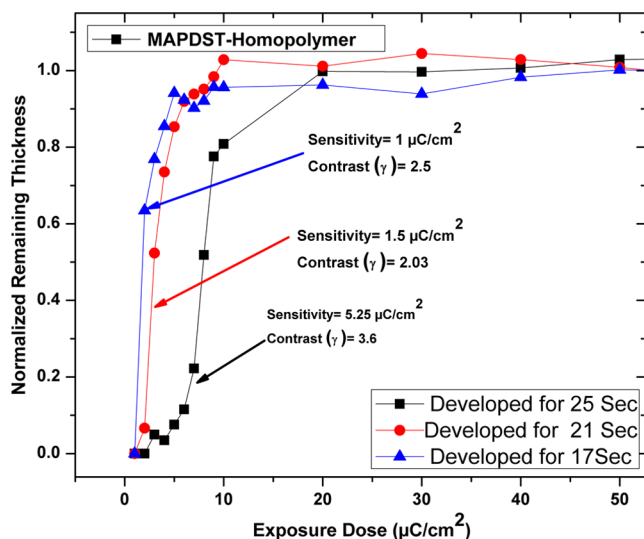
Fig. 3 NRT response curves of nonchemically amplified resist (MAPDST homopolymer) processed for different development times while keeping other conditions the same, i.e., postexposure bake (PEB), postapply bake (PAB), and exposure conditions.
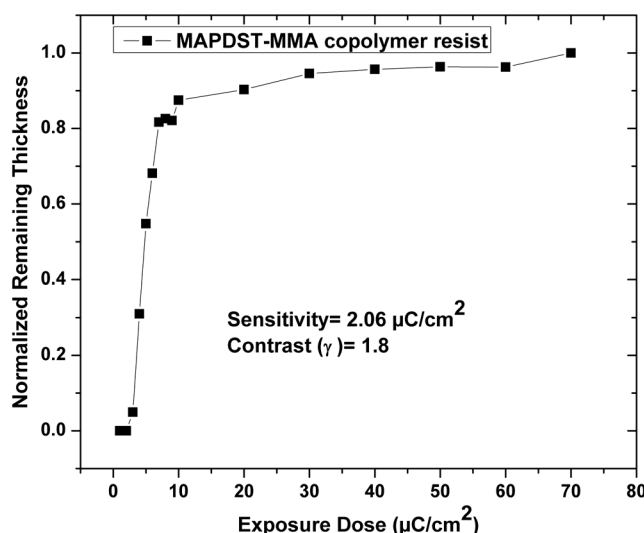

Fig. 4 Sensitivity to electron dose characteristics for MAPDST-MMA copolymer.

Fig. 5 (a) Surface roughness (rms value) of MAPDST homopolymer with E-beam exposure dose under same conditions, i.e., PEB/PAB, and same developing condition.

3.5 Polarity Switching Mechanism

As discussed in the previous sections, the unexposed polymer thin film is polar and actually highly hydrophilic in nature because of its strong ionic character. Therefore, it is soluble in polar solvents such as water. Upon exposure to radiation, the polymer undergoes a polarity change making the exposed area less polar than the unexposed area, which in turn brings on differences in solubility of these exposed and unexposed areas. Thus, when irradiated, the anionic counter ions ($CF_3SO_3^-$) of the resists decomposed resulting in the formation of Ar-S^+-$(CH_3)_2$ groups, which upon postbake annealing, get converted to Ar-S-CH_3 (nonionic in nature). This was confirmed from EUV photodynamic studies, which are discussed in detail in the next section. As the exposed polymer thin film lost its ionic character, it became less polar and was found to be insoluble in polar solvents. The unexposed regions of the resist film were readily soluble in optimized TMAH solution in DI-water, and the exposed regions (patterns) were intact when dipped into the developer, establishing its nature as a unique negative tone photoresist.

3.6 EUV Photodynamic Studies of n-CARs Formulation

The photosensitivity analysis of these n-CARs, MAPDST homopolymer, and MAPDST-MMA copolymer formulation was executed to inspect the precise chemical information and photochemistry of synthesized resist materials. The MAPDST homopolymer and MAPDST-MMA copolymer thin films were irradiated at 103.5 eV at selected fixed periods of time. During irradiation, the volatile ion fragments, measured by an *in situ* gas analysis, desorbed from the polymer surfaces after continuous SR excitation. Figure 8 shows the time evolution of SO_2^+, SO^+, and CF_3^+ fragments during irradiation of the MAPDST-MMA copolymer. Hydrocarbons were also observed as background gases in the UHV chamber. One of them is the $C_5H_9^+$ fragment coincident with the CF_3^+ ion. In our previous publication,[16] it was found that in the case of the MAPDST homopolymer, SO_2^+ and SO^+ intensities increased to reach a maximum and then decreased

(sensitivity ~30 mJ/cm^2) and the MAPDST-MMA copolymer (sensitivity 10 mJ/cm^2) as shown in Fig. 6. The calculated 3σ LER of the 20-nm lines for the MAPDST homopolymer (exposure dose 94 mJ/cm^2) and the MAPDST-MMA copolymer (exposure dose 33 mJ/cm^2) are 2.0 ± 0.3 and 1.8 ± 0.1 nm, respectively (LER was calculated as the average of the edge roughness of 10 lines). In addition to line patterns, we also attained complex patterns, such as circular L/S patterns (Fig. 7), further supporting the potential of these resist materials for the most promising EUV technology. Such circular complex features are for potential applications in diffraction grating. We, therefore, strongly believe these materials will provide a path forward for designing n-CARs that may attain higher resolutions than current CARs at competitive sensitivities.
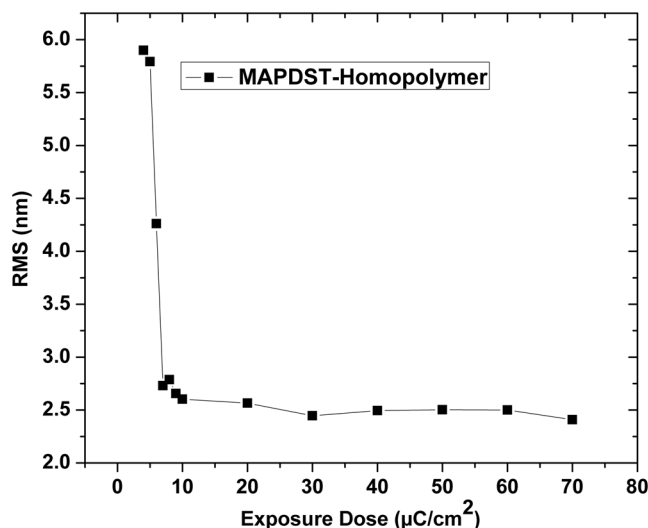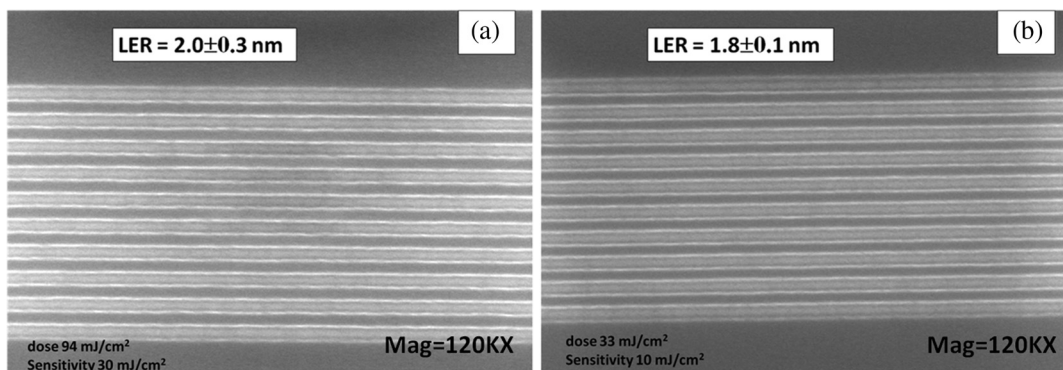
Fig. 6 High-resolution extreme ultraviolet (EUV) exposure results of 20-nm lines with L/S patterns of nonchemically amplified (a) MAPDST homopolymer and (b) MAPDST-MMA copolymer resists.
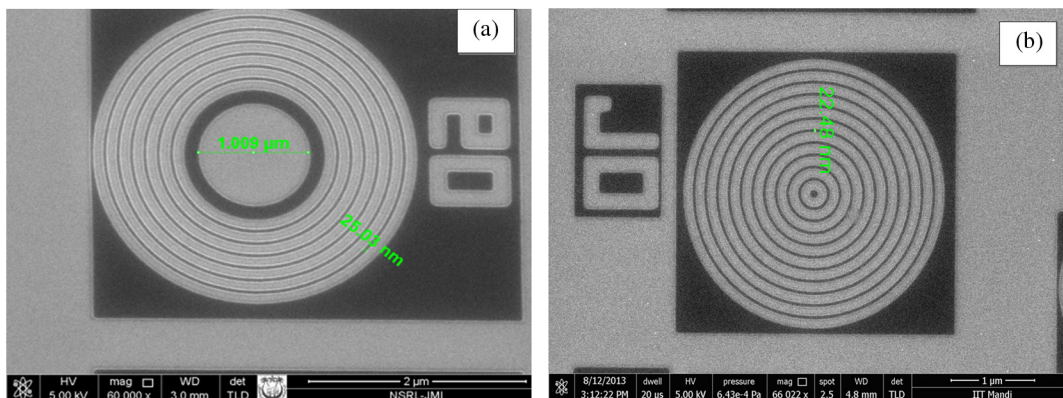

Fig. 7 EUV exposure results on circular patterns: 25 nm circular patterns of MAPDST homopolymer resist (a) and 22 nm circular patterns of MAPDST-MMA copolymer resist (b).

to zero in a few minutes; the $m/z = 69$ increased to a maximum and then decreased to the background level. The new contribution of $m/z = 69$ observed corresponds to the desorption of CF_3^+ ions produced by 103.5 eV photon excitation. The results showed that irradiation of the MAPDST homopolymer films produced a fast desorption process where a maximum in the QMS signal intensity is reached between 10 and 15 s.[16] On the contrary, excitation at 103.5 eV of MAPDST-MMA copolymer films yielded a lower QMS signals and the maximum of the intensity is reached at longer times (~100 s, see inset of Fig. 8). Because the SR beam current for both experiments was almost the same (~210 mA), it is possible to infer that the MAPDST-MMA copolymer is more resistant to radiation damage with a lower degree of degassing. This can be attributed to the copolymer microstructure where methyl methacrylate units replace the more volatile sulfonium moieties. To confirm the above QMS results, high resolution x-ray photoelectron spectroscopy (HR-XPS) spectra were obtained at the C 1s and S $2p$ excitations. Figure 8 shows that after 5 min of irradiation of the MAPDST-MMA copolymer film at 103.5 eV, C—O, COO, and CF_3 signals still remained on the surface of the polymer. The resistance to radiation of the MAPDST-MMA copolymer contrasted with the photofragmentation dynamic of the MAPDST homopolymer.[16] Only 1 min of irradiation of the MAPDST homopolymer at 103.5 eV led almost to the disappearance of the COO signal intensity together with a strong decrease in the CF_3 signal.
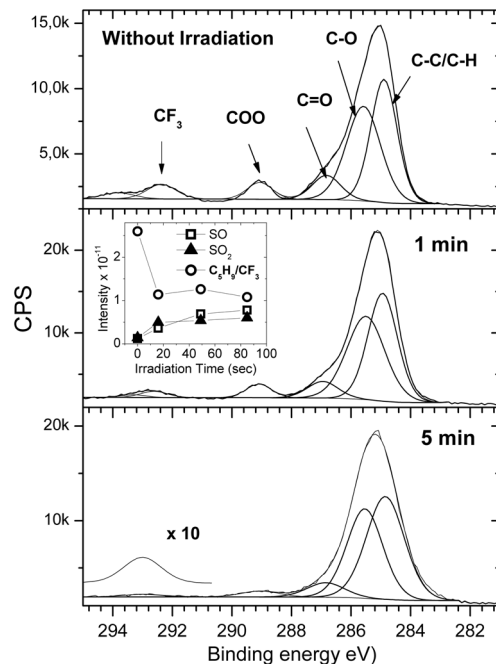

Fig. 8 High-resolution x-ray photoelectron spectroscopy (XPS) spectra of the C 1s envelope of the MAPDST-MMA copolymer films before irradiation and after 1 and 5 min of SR irradiation at 103.5 eV. Inset: *in situ* quadruple mass spectrometer gas analysis during irradiation of the films at 103.5 eV of excitation energy.

Additionally, no detection of both signal contributions was observed at 5 min of irradiation. Interestingly, the main C 1s signals (C─C/C─H, C═O, and C─O contributions) in the MAPDST-MMA copolymer seemed not to be affected after irradiation. This result contrasted with the MAPDST homopolymer where new functionalities were needed to incorporate in the deconvolution to obtain a right fit after irradiation.[16] The C 1s XPS results match the QMS ones showing that an MAPDST-MMA copolymer may have a higher stability under 103.5 eV SR radiation excitation.

The analysis of the HR-XPS results of S 2p signals give more detailed information about the polymer's stability against the SR radiation (Fig. 9). The MAPDST homopolymer loses sulfur components rapidly and after 5 min of irradiation at 103.5 eV, the only contribution left is the S-C bonding, probably belonging to the (dimethylthio)phenyl group.[16] The MAPDST-MMA copolymer again looked more stable and mainly lost the S═O contribution. The QMS, C 1 s, and S 2p XPS results allow confirmation that the copolymer is more resistant to 103.5 eV radiations than the MAPDST homopolymer with a lower degree of degassing during irradiation in the case of the MAPDST-MMA copolymer.

L-near edge x-ray absorption fine structure (NEXAFS) spectroscopy is sometimes more sensitive to geometrical and chemical changes in the top most monolayers of a material than the K-inner shell excitations. L-edge sulfur NEXAFS spectroscopy was investigated to better understand the XPS and QMS results in relation to the high radiation resistance of the MAPDST-MMA copolymer. The inset of Fig. 10 shows the untreated NEXAFS spectra of the MAPDST-MMA copolymer. Three main signals, labeled as A, B, and C, can be identified in the pristine film. Comparison with previous results of gas phase SO_2 and polymer samples[23–25] allows interpretation of the signal A to electronic transitions involving the spin-orbit split of the $2p$ sulfur excited species ($2p_{1/2}$ and $2p_{3/2}$ levels) mainly to the unoccupied π^* antibonding orbitals. Signal B may correspond to the mixture of $2p_{1/2} \rightarrow \pi^*$, $2p_{3/2} \rightarrow \sigma_{(C–S)}$, $2p_{1/2} \rightarrow \sigma_{(C–S)}$, and S $2p \rightarrow$ empty S 3d transitions that cannot be resolved. Finally, signal C can also be assigned to
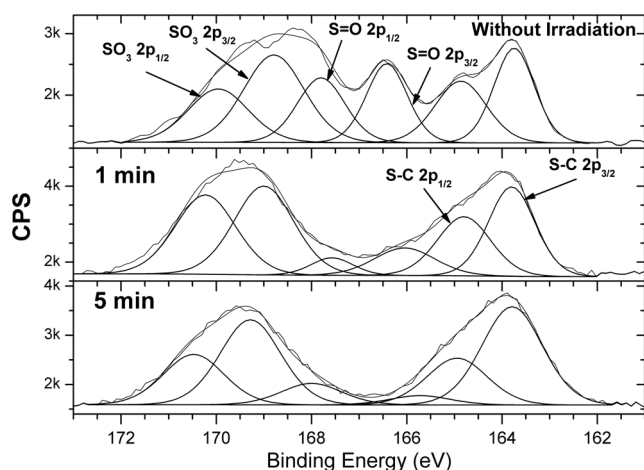

Fig. 9 High-resolution XPS spectra of the S $2p$ envelope of the MAPDST-MMA copolymer films before irradiation and after 1 and 5 min of SR irradiation at 103.5 eV.
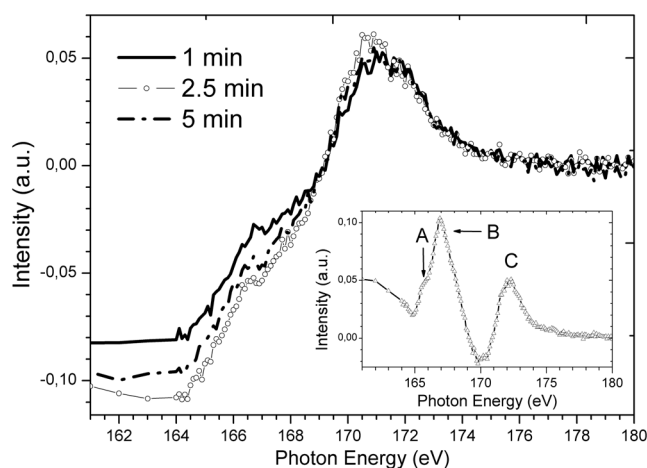

Fig. 10 L-near edge x-ray absorption fine structure (NEXAFS) spectra of the untreated MAPDST-MMA copolymer (inset) along with their difference spectra "irradiated minus untreated spectrum." Irradiation times at 103.5 eV are indicated in the figure.

higher energy S $2p \rightarrow$ empty S 3d transitions and S $2p \rightarrow \pi^*_{(S═O)}$ sulfonic acid functionalities. To clearly see the effect of the radiation on the MAPDST-MMA copolymer, Fig. 10 shows the difference spectra between each irradiated film and the untreated spectra (inset of Fig. 10). As can be seen in Fig. 10, signals A and C resisted the irradiation and signal B had already disappeared in the first minute of irradiation. Because signal B is a mixture of several transitions, it can be hypothesized that the MAPDST-MMA copolymer may develop a rearrangement during irradiation that finally maintained the S─C and SO_x functional groups almost intact (there were no important shifts in energies in the A and C signals). The energy resolution of the beam line did not allow the separation of each contribution in the NEXAFS spectra. On the contrary, the sulfur NEXAFS spectra of the irradiated MAPDST homopolymer (Fig. 11) showed that signal B resisted the irradiation and signal C shifted to higher energies in ~2 eV. The new signal of C = 176.8 eV can be assigned to a transition from S $2p$ to the empty S 3d (t_2 states) and multiple high energy scattering,[24] i.e., losing the SO_3 functionality.

From the above photodynamic data, it can be concluded that for a polarity change for the copolymer on EUV exposure, compared to the homopolymer,[16] fewer sulfonyl groups are affected since the hydrophobic MMA groups function as dissolution inhibitors. Further evidence is provided by the higher sensitivity of the copolymer to EUV photons ~10 mJ/cm^2 compared to ~30 mJ/cm^2 for the homopolymer.

3.7 AFM Analysis

Finally, the AFM analysis of the copolymer EUVL features was explored as there is more confidence in the exposure dose and subsequent exposure conditions.

The AFM integrated with a diamond needle (cantilever) tip was used for metrology investigations of the MAPDST-MMA copolymer n-CAR. The radius of curvature of the tip apex and spring constant of the cantilever were 1 nm and 20 to 50 N/m, respectively. The internal topography for the 20-nm line pattern features could not be imaged satisfactorily because the tip was touching the walls of the 20 nm features due to the fast scan speed of the AFM system.
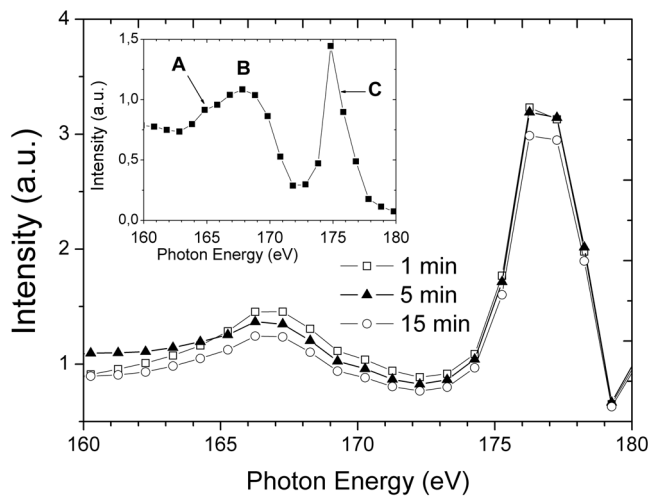
Fig. 11 NEXAFS spectra of the untreated MAPDST homopolymer (inset) along with their difference spectra "irradiated minus untreated spectrum." Irradiation times at 103.5 eV are indicated in the figure.

Figures 12(a) and 12(b) represent the AFM images of the surface 2.4×2.4 μm. While imaging with a slow scan speed (0.5 Hz with 512 points along the x-line), sufficient resolution was obtained. Though the tip successfully revealed that the pattern width is 20 nm, it could not reach to the bottom of each pattern and, therefore, did not show the internal structure of the pattern walls. Indeed, sometimes it was observed that the tip was touching the inner walls of the 20-nm-wide patterns. Due to the small distance at the inner space of the pattern, the tip reached the other side of the inner wall before touching the bottom of the patterns. In order to have a clear idea about the actual shape of the pattern up to the bottom of the polymer layer, smaller segments of the polymer surface were scanned, such as the one shown in Fig. 12(c) (1.25 μm $\times$ 1.25 μm). Note that this pattern is not 20 nm wide, it is wider and in the range of 50 to 60 nm as can be seen at the cross-section. We could reach to the bottom because of this larger space and detect that the polymer is 43.5 nm thick. This helped in the imaging of well-developed patterns with regular and expected shapes.

Figure 12(b) shows the three-dimensional images of the MAPDST-MMA copolymer resist patterns, which signify the regular space 25 nm (left) and 20 nm (right) of the resist lines and high aspect ratio of the MAPDST-MMA copolymer developed line patterns. Additionally, it reveals very good adhesion between the MAPDST-MMA copolymer negative tone resist and the silicon substrate. Therefore, it indicates that the MAPDST-MMA copolymer line patterns have the required adhesion strength. The depth profile analysis and section investigation of Fig. 12(c) confirm that the well-developed lithographic patterns possess a depth of 45 to 50 nm, matching the MAPDST-MMA copolymer resist film thickness (40 to 50 nm). It is noted that the MAPDST-MMA negative tone copolymer resist line patterns are fully developed up to the silicon surface.

3.8 Etch Resistance

The etch chemistry of SF_6 was used to characterize the nonchemically amplified MAPDST homopolymer and MAPDST-MMA copolymer resists. The thicknesses of the films were
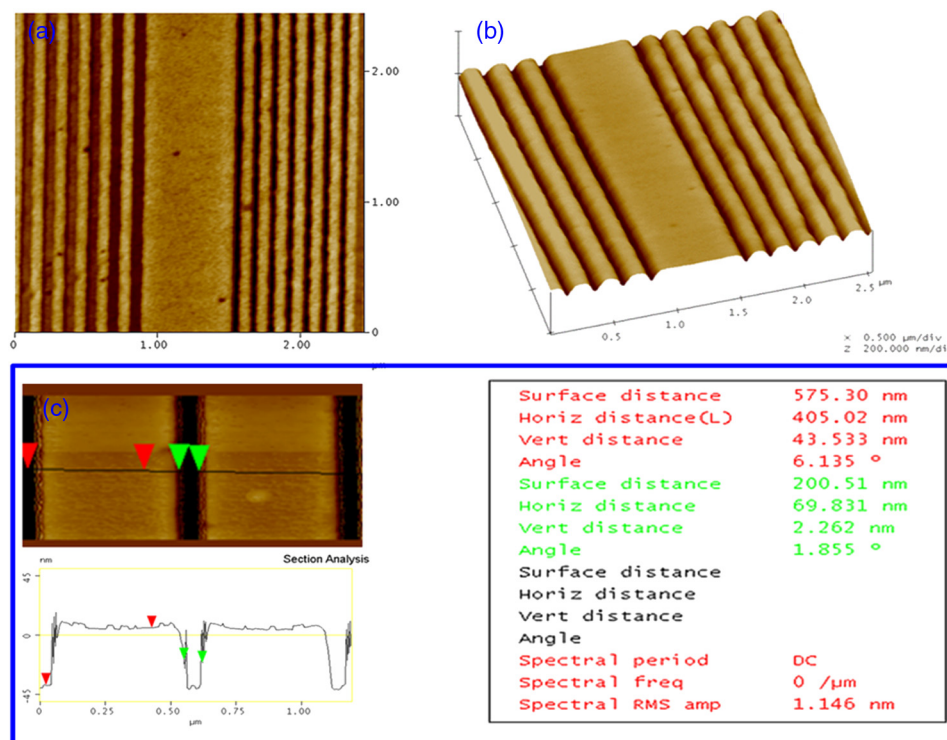

Fig. 12 (a) Atomic force microscope surface topography image of 2.4×2.4 μm area for nonchemically amplified MAPDST-MMA copolymer resist. (b) Three-dimensional images of MAPDST copolymer resist patterns with the regular space 25 nm (left) and 20 nm (right). (c) The depth profile analysis and section investigation.
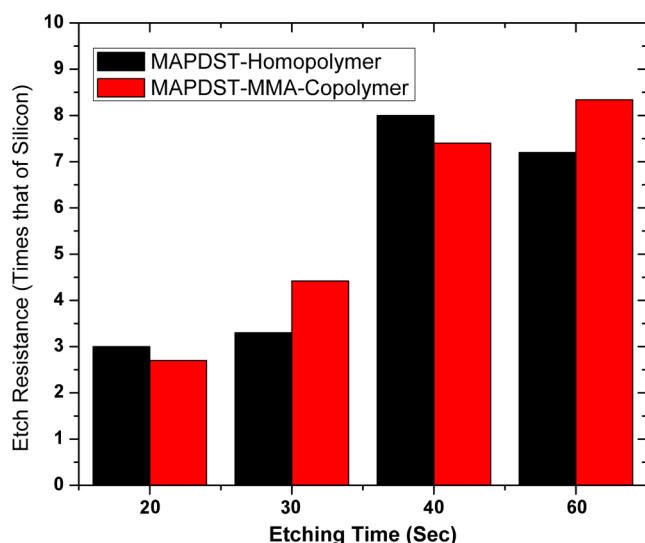
Fig. 13 Etch resistance to plasma etching of MAPDST homopolymer and MAPDST-MMA copolymer resists (under SF_6 plasma chemistry) relative to the etch resistance of silicon.

measured before and after reactive ion etching by Bruker's DektakXT™ (Santa Barbara, California) Stylus Profilometer. The recipe for plasma etching was SF_6 at a flow rate of 5 sccm and a pressure of 10 mTorr with an RF power of 20 W for 20, 30, 40, and 60 s for both resist materials. The etch ratios of the MAPDST homopolymer and MAPDST-MMA copolymer resists with respect to the silicon substrate were 7.2:1 and 8.3:1, as shown in Fig. 13. These materials show a very high etch resistance to the silicon substrate when compared to conventional organic resists.[22–27] The MAPDST-MMA copolymer was also tested under an etch recipe of CHF_3/O_2 with a flow rate of 22.5/2.5 sccm at a pressure of 80 mTorr with an RF power of 150 W for 1 min. In this case, the etch ratio for the MAPDST-MMA copolymer to the silicon dioxide was observed as 0.36:1, which is also comparable to conventional organic resists under the same conditions.[28]

4 Conclusions

To conclude, the e-beam lithography and EUVL investigations of two novel resists, MAPDST homopolymer and MAPDST-MMA copolymer, demonstrated their high performance capabilities resolution down to 20 nm with higher contrast ratio (γ) of 3.6 and 1.8 under e-beam lithography and etch resistance (under SF_6 plasma chemistry) with respect to silicon substrate are 7.2:1 and 8.3:1, respectively. EUV lithography shows similar resolution and good sensitivity. Further detailed study is needed to optimize these n-CAR materials for EUV lithography patterning applications for a sub-20 nm node. However, present EUV/e-beam lithography results demonstrate their excellent performance characteristics, showing low line edge roughness compared with existing chemical amplified resist materials. Further improvement toward sensitivity of these materials is underway in order to achieve high resolution line patterns down to 11 nm L/S features with low line edge roughness. We are also exploring the possibility of the incorporation of dark elements in the polymer backbone microstructure to increase EUV photon absorption capability, which might lead to an increase in sensitivity.

References

1. TWINSCAN NXE:3300B, http://www.asml.com/asml/show.do?lang=EN&ctx=46772&dfp_product_id=842 (30 July 2014).
2. "The international technology roadmap for semiconductors," REPORTS' SUMMARIES/Lithography, http://www.itrs.net/Links/2013ITRS/Summary2013.htm (21 August 2014).
3. J. W. Thackeray, "Materials challenges for sub-20-nm lithography," *J. Micro/Nanolith. MEMS MOEMS* **10**(3), 033009 (2011).
4. P. P. Naulleau et al., "Critical challenges for EUV resist materials," *Proc. SPIE* **7972**, 797202 (2011).
5. W. Yayi et al., "Performance of chemically amplified resists at half-pitch of 45 nm and below," *Proc. SPIE* **6519**, 65190R (2007).
6. I. B. Baek et al., "Electron beam lithography patterning of sub-10 nm line using hydrogen silsesquioxane for nanoscale device applications," *J. Vac. Sci. Technol. B* **23**(6), 3120–3123 (2005).
7. H. Tsubaki et al., "EUV resist materials design for 15 nm hp and below," *Proc. SPIE* **8679**, 867905 (2013).
8. K. Cho et al., "EUV patterning results at SEMATECH," in *Int. Symp. on Extreme Ultraviolet Lithography*, Vol. 1, p. 1001, Curran Associates, Inc. (2012).
9. Y. Ekinei et al., "Evaluation of EUV resist performance with interference lithography towards 11 nm half-pitch and beyond," *Proc. SPIE* **8679**, 867910 (2013).
10. C. Anderson et al., "The SEMATECH Berkeley MET: demonstration of 15-nm half-pitch in chemically amplified EUV resist and sensitivity of EUV resists at 6.x-nm," *Proc. SPIE* **8322**, 832212 (2012).
11. V. Singh et al., "Towards novel non-chemically amplified (n-CARS) negative resists for next generation lithography (NGL) applications," *J. Mater. Chem. C* **2**, 2118–2122 (2014).
12. K. E. Gonsalves et al., "Organic-inorganic nanocomposites: unique resists for nanolithography," *Adv. Mater.* **13**, 703–714 (2001).
13. K. E. Gonsalves and H. Wu, "A novel single-component negative resist for DUV and electron beam lithography," *Adv. Mater.* **13**, 195–197 (2001).
14. K. E. Gonsalves, "High resolution resists for next generation lithographies," U.S. Patent 7 008 749 B2 (2006).
15. A. A. Brown et al., "Polymer brush resist for responsive wettability," *Soft Matter* **5**, 2738–2745 (2009).
16. V. S. V. Satyanarayana et al., "Radiation sensitive novel polymeric resist materials: iterative synthesis and their EUV fragmentation studies," *ACS Appl. Mater. Interfaces* **6**, 4223–4232 (2014).
17. V. Canalejas-Tejero et al., "Ultrasensitive non-chemically amplified low-contrast negative electron beam lithography resist with dual-tone behaviour," *J. Mater. Chem. C* **1**, 1392–1398 (2013).
18. The SEMATECH Berkeley Microfield Exposure Tool (MET), http://met.lbl.gov/ (4 December 2013).
19. "Information and data sheets," http://www.allresist.de (March 2012).
20. "Information and data sheets," http://www.microresist.com (March 2012).
21. A. E. Grigorescu and C. W. Hagen, "Resists for sub-20-nm electron beam lithography with a focus on HSQ: state of the art," *Nanotechnology* **20**(29), 292001 (2009).
22. F. Gibbons et al., "A chemically amplified fullerene derivative molecular electron beam resist," *Small* **3**(12), 2076–2080 (2007).
23. B. W. Yates and D. M. Shinozaki, "Radiation degradation of poly (butene-1 sulfone) and poly(1,4-phenylene ether sulfone) in the soft x-ray region," *J. Mater. Res.* **7**(2), 520–524 (1992).
24. E. Cortes et al., "Perchloromethyl mercaptan, CCl3SCl, excited with synchrotron radiation in the proximity of the sulfur and chlorine 2p edges: dissociative photoionization of highly halogenated species," *J. Phys. Chem. A* **113**(35), 9624–9632 (2009).

25. Q. Lud et al., "Controlling surface functionality through generation of thiol groups in a self-assembled monolayer," *Langmuir* **26**(20), 15895–15900 (2010).
26. Y. Jinxing et al., "Novel ester acetal polymers and their application for positive-tone chemically amplified i-line photoresists," *J. Mater. Chem. C* **1**(6), 1160–1167 (2013).
27. M. Trikeriotis et al., "A new inorganic EUV resist with high-etch resistance," *Proc. SPIE* **8322**, 83220U (2012).
28. M. A. Ali et al., "A new nanocomposite resist for low and high voltage electron beam lithography," *Microelectron. Eng.* **70**(1), 19–29 (2003).

Vikram Singh is presently working as a research scientist in an INTEL USA funded project at the Indian Institute of Technology (IIT) Mandi, Himachal Pradesh, India. He is focusing on nonchemically amplified resists for extreme ultraviolet lithography (EUVL) at the 10-nm node and beyond. He wrote his PhD thesis on the topic fabrication, characterization, and reliability study of HfO_2 high-k gate dielectric for advanced CMOS technology in 2012 from the Electronics Science Department, Kurukshetra University.

Vardhineedi Sri Venkata Satyanarayana received his PhD in the field of synthetic organic chemistry from VIT University, Vellore, India, in 2011. He has good hands-on experience in organic synthesis and materials synthesis. Presently, he is working for a project funded by INTEL Corp., USA, as a research scientist (PDF) at IIT Mandi, Himachal Pradesh. He is working on the design and synthesis of nonchemically amplified resists for EUVL at sub-20 nm half pitch.

Nikola Batina is a full professor of chemistry at the Department of Chemistry, Universidad Autonoma Metropolitana-Iztapalapa (UAM-I), Mexico City, Mexico. He is a (co)author of over 120 publications in refereed international journals and supervisor of 11 PhD dissertations. He has had research programs on atomic and nanometer-resolution surface science, electrochemistry, and nanotechnology. He is the founder and leader of the Nanotechnology and Molecular Engineering Laboratory.

Israel Morales Reyes is a PhD student at the Biomedical Engineering School at UAM-I, Mexico City, Mexico. He received his bachelor's degree in mechatronics engineering from Unidad Profesional Interdisciplinaria en Ingeniería y Tecnologías Avanzadas (Mexico City) and his master's degree in biomedical engineering (honors) from UAM-I, Mexico City. His interest and work are focused on carbon nanotubes electronics, neural cells electrophysiology, and nanomaterial characterization by atomic force microscope and STM.

Satinder K. Sharma earned his PhD from the Department of Electronics Science, Kurukshetra University, India, in 2007 followed by postdoctoral studies at IIT Kanpur. He served IIIT Allahabad as a faculty member during 2010 to 2012. He is currently an assistant professor in the School of Computing and Electrical Engineering at IIT Mandi. His current research interests include microelectronic circuits and systems, CMOS device fabrication and characterization, nanoelectronics, nano/microfabrication and design, polymer nanocomposite, and sensors, photovoltaic and self-assembly.

Felipe Kessler holds a degree in chemistry from Regional Integrated University of High Uruguay and Missions, a master's degree in chemistry from the Federal University of Rio Grande do Sul (UFRGS), and a PhD in chemistry from UFRGS. He carried out a one-year doctoral period in the University of Manchester, United Kingdom, and now is in a postdoctoral position at Makenzi University, Brazil. He has experience in the fields of chemistry, physical chemistry of surfaces, and photochemistry.

Francine R. Scheffer holds a degree in chemistry from the Federal UFRGS and a master's degree in material science from UFRGS. She has experience in physical chemistry, photocatalysts, and hydrogen photogeneration by the water-splitting reaction.

Daniel E. Weibel studied chemistry (diploma) at the Nacional University of Córdoba (UNC) and obtained a PhD in physical chemistry from UNC. He spent postdoctoral periods at the University of Gakusuin, Japan, Munster University, Germany, and Manchester University, United Kingdom. He is currently an associate professor at UFGRS, Brazil. He has experience in the field of physical-chemistry and, in particular, in surface science acting on the following topics: TOF-SIMS, x-ray photoelectron spectroscopy, AES, L-near edge x-ray absorption fine structure, synchrotron radiation, polymers, and photochemistry.

Subrata Ghosh received his PhD from IIT Guwahati followed by postdoctoral studies at Bar-Ilan University, Israel, Case Western Reserve University, USA, and University of Leipzig, Germany. He is the recipient of the Alexander von Humboldt Fellowship. Currently, he is working as an assistant professor at IIT Mandi. While he is looking at the applications of newly developed soft materials as molecular markers to understand various biological events, he is equally interested in developing materials for electronic applications.

Kenneth E. Gonsalves is a visting distinguished professor at IIT Mandi, Himachal Pradesh, India. He was the Celanese-Acetate distinguished professor at the University of North Carolina at Charlotte. His research has focused on the development of new resists for EUVL as well as resists for bionanotechnology applications. His emphasis is on polymer materials synthesis, including nanomaterials.